

An occult urothelial carcinoma with wide multiorgan metastases and its genetic alteration profiling

Case report and literature review

Kunpeng Bu, MM^a, Zeyan Shi, MM^b, Yang Lu, MM^a, Juan Zhao, MS^c, Bixun Li, MM^{a,*}

Abstract

Rationale: Urothelial carcinoma, also named transitional cell carcinoma, is the most frequent occurring malignancy in the urinary system. It mainly invades the surrounding tissues and metastasizes to distant organs in later stages.

Patient concerns: Here, we presented an unusual case of occult urothelial carcinoma primarily manifested as a multiorgan metastatic cancer in a 59-year-old man. The patient complained of pain on the left thigh root for a month. The imaging and histopathological examination revealed multiple malignancies in lung, bone, and liver.

Diagnoses: The histological evaluation and the immunohistochemistry (IHC) profile of liver, lung, and bone were consistent with the diagnosis of metastases from the original urothelial cancer, while imaging examination was not able to detect a primary lesion in the urinary system.

Interventions: Based on the mutation of *STK11* M51fs*106 detected by next generation sequencing (NGS), we started targeted therapy with everolimus.

Outcomes: The patient deteriorated after 3 months of treatment and passed away.

Lessons: In this initial report of occult urothelial carcinoma, we obtained information on genetic variations of tumor tissue which could provide important information for subsequent studies on this kind of disease.

Abbreviations: CA = carbohydrate antigen, CEA = carcinoembryonic antigen, CK = creatine kinase, CUP = carcinoma of unknown primary, CVT = clinical target volume, ECT = emission CT, GATA3 = GATA binding protein, GTV = gross tumor volume, HGF = hepatocyte growth factor, Hh = Hedgehog, IHC = Immunohistochemistry, NGS = next generation sequencing, NMD = nonsense-mediated mRNA decay, PAX-8 = paired-box-8, pCTV = prophylactic CTV, PD = progressive disease, PR = partial response, PTCs = premature termination codons, RECIST = response evaluation criteria in solid tumors, SCC = squamous cell carcinoma associated antigen, SD = stable disease, T-PSA = total prostatic specific antigen, TTF-1 = thyroid transcription factor-1.

Keywords: genetic mutation profiling, multiorgan metastasis, occult urothelial carcinoma

Editor: N/A.

Patient Consent: We ensure that the patient's privacy is protected. Informed consent for publication of the case has been obtained in writing from the deceased patient's next of kin.

The author of Juan Zhao is an employee of Origimed, and other authors have no conflicts of interest to disclose.

^a Department of Comprehensive Internal Medicine, The Affiliated Tumor Hospital of Guangxi Medical University, Nanning, ^b Department of Hematology, First Hospital Affiliated to Guangxi Medical University, Guangxi, ^c Origimed, Shanghai, China.

* Correspondence: Bixun Li, Department of Comprehensive Internal Medicine, The Affiliated Tumor Hospital of Guangxi Medical University, #71 Hedi Road, Nanning, Guangxi Province, 530021, China (e-mail: li4738@163.com).

Copyright © 2019 the Author(s). Published by Wolters Kluwer Health, Inc. This is an open access article distributed under the terms of the Creative Commons Attribution-Non Commercial-No Derivatives License 4.0 (CCBY-NC-ND), where it is permissible to download and share the work provided it is properly cited. The work cannot be changed in any way or used commercially without permission from the journal.

Medicine (2019) 98:16(e15245)

Received: 18 October 2018 / Received in final form: 7 March 2019 / Accepted: 20 March 2019

<http://dx.doi.org/10.1097/MD.00000000000015245>

1. Introduction

In the diagnosis and treatment of cancers, it is essential to identify the source of tumor cells because this determines treatment options. Occult cancer is quite rare and defined as a clinically unknown malignancy in which the primary lesion is difficult to identify. The apparent metastatic tumor is diagnosed by clinicians and pathologists according to histological examination. For some patients, the micro primary carcinoma can be detected when a patient is being evaluated for autopsy.^[1] To date, most occult cancers have been reported in breast cancer and a few in thyroid and gynecologic cancers.^[1-4] Also, a few occult somatic malignant tumors may also present acute cerebral infarction as the first clinical manifestation.^[5,6] The occurrence of occult cancer is so rare that it only accounts for about 0.3% to 1.0% of all newly diagnosed breast cancer cases.^[7,8]

Urothelial carcinoma, which is also known as transitional cell carcinoma, is a malignant tumor that arises from the transitional epithelium. It commonly occurs in the urinary tract. Metastasis of urinary tract cancer to distant organs is rare and usually occurs in advanced stages after diagnosis. To date, the initial clinical manifestation of urothelial carcinoma as metastasis has not been reported. Here, we present an unusual case of occult urothelial

cancer which manifested in multiorgan metastasis including lung, liver, and bone at an early stage.

2. Case presentation

The patient was a 59-year-old man who complained of continuous acupuncture-like pain (VAS score of about 8) for a month which started on April 10, 2017 in the left upper thigh. There was no visible lesion on the local skin and the pain did not radiate or affect movement, and therefore, no treatment was given. A month later, the pain gradually worsened and began to radiate toward the sacrococcygeal region and the right buttocks, and increased when the patient was walking. The patient had a history of smoking 20 cigarettes per day and drinking 1 to 1.5 mL of alcohol a week for about 20 years. No positive found in family history. The patient went to a local hospital for medical care on May 22, 2017. Computed tomography (CT) examination showed space-occupying lesions on the tip of the upper lobe of the right lung, a few small lymph nodes in the mediastinum, multiple locations of bone destruction on the body and pedicle of L4 lumbar vertebra, and space-occupying lesions with slightly low density on the left lateral lobe of the liver (Fig. 1). The abnormal images of the lung, mediastinum, liver, and bone were all considered highly probable malignant lesions (either primary or metastatic) by radiologists. Further examination was recommended to make a clear diagnosis.

The patient went to our hospital for further medical care on May 27, 2017. Tumor markers were detected as follows: total prostatic specific antigen (T-PSA) 0.55 ng/mL (normal: 0–4), carcinoembryonic antigen (CEA) >100.00 ng/mL (normal: ≤5 ng/mL), carbohydrate antigen 125 (CA-125) 46.8 U/mL (normal: ≤35 U/mL), CA-153 157.8 U/mL (normal: ≤31.3 U/mL), and squamous cell carcinoma associated antigen (SCC) 4.64 ng/mL (normal: 0–1.5 ng/mL). CT results showed a right lung upper lobe mass shadow with size of about 3.1 × 2.5 cm, 4 to 6 small lymph nodes in the mediastinum and multiple low-dense nodules in the thyroid gland. CT reconstruction bone window showed bone destruction of the right fourth rib, L4 vertebral body, and bilateral iliac with soft tissue mass formation. Slightly low-density nodules (3.0 × 2.5 cm) in the left lateral lobe of the liver were slightly enhanced on contrast, and multiple low-density nodules were found in other regions of the liver parenchyma (Fig. 2). No abnormalities were found in gallbladder, bile duct, spleen, pancreas, kidneys, adrenal glands, bladder, or rectum. Whole body bone emission CT (ECT) imaging on June 1, 2017 showed multiple abnormal concentrations of radioactivity on both sides of the ilium. The skeletal radioactive distribution in the

skull, sternum, clavicle, scapula, spine, ribs, limbs, and other parts were uniform and symmetrical. The active metabolism of bilateral iliac bone was considered to be possible metastases (Fig. 3). Pelvic magnetic resonance imaging (MRI) showed bone destruction with soft tissue mass formation on bilateral iliac and upper femur segments, and showed iso signal intensity in a T1-weighted image and heterogeneous slightly high signal intensity in a T2-weighted image (Fig. 4). Combined with medical history, it was considered to be possible bone metastases.

Although all previous examinations suggested the possibility of malignancy, they were still insufficient for diagnosis. For confirmation, biopsies were done with the consent of the patient. In the days following, the left iliac, liver, and pulmonary were punctured under the guidance of B-mode ultrasonography. Representative pictures of pathological examination of each specimen are showed in Fig. 5. The pathological evaluation of bone, liver, and lung suggested a high-grade metastatic urothelial carcinoma. Based on results of bone IHC, (Creatine Kinase) (CK) 5/6+ scattered, CK7+, GATA binding protein 3 (GATA3)+, P40+ few, CK20-, Villin-, thyroid transcription factor-1 (TTF-1)-, CDX2-, Glypican3- and Alpha-1 Antitrypsin (AAT)+ few, liver IHC (CK7+, CK20-, Villin-, TTF-1-, paired-box-8 (PAX-8)-, GATA-3-, CDX-2+, Ki-67+ about 60%), and lung IHC (CK5/6-, P40-, CK20-, GATA-3+ partial, CK7+ strong and widespread, TTF-1-, NapsinA-, Ki-67+ 40%), it did not support adenocarcinoma or squamous cell carcinoma from lung, liver, intestines, or stomach. In conclusion, combining the images of the hematoxylin and eosin (H&E) staining and IHC staining, all tumor tissues most likely came from urothelium tissue rather than lung or digestive system tissue. On June 22, 2017 after a multidisciplinary consultation, the patient was diagnosed with occult urothelial carcinoma with bone, liver, and lung metastases, without primary urinary tract lesions.

After some pretreatment preparation, the patient began to receive radiotherapy on July 4, 2017. Target delineation: CT imaging of lumbar and pelvic tumors were gross tumor volume (GTV)1 and GTV2, respectively. The vertebral tumor and the appendage of GTV1 was clinical target volume (CTV)1. CTV2 included GTV2 expanded 1 cm and the imaging of the area of muscle edema. CTV1 externally expanded 5 mm was prophylactic CTV (pCTV)1. CTV2 expanded 1 cm on top and bottom, and 5 mm in other directions was PCTV2. The dose of irradiation was pCTV1: 33.8 Gy/13f, pCTV2: 39 Gy/13f. One week later, the patient expressed relief of pelvic bone pain, but had worse pain in the right rib. CT results suggested progressive disease (PD). Since the tumor of the ribs and cervical vertebrae were close to the spinal cord and liver tumors had increased in size, the

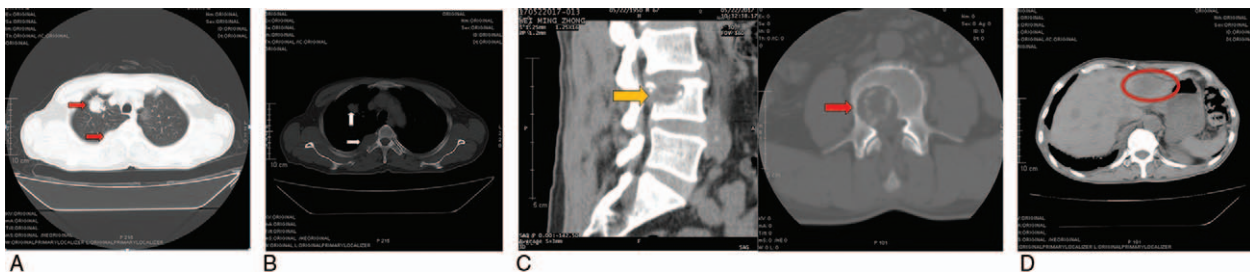


Figure 1. CT examination in local hospital on May 22, 2017. A. Lung window in CT scan of a space-occupying focus on the tip of the upper lobe of the right lung. B. Mediastinal window in CT scan of a space-occupying focus on the tip of the upper lobe of the right lung. C. CT scan of the fourth lumbar spine destruction. D. CT scan of a space-occupying lesion on the left lobe of the liver with a size of about 3.0 × 2.4 cm. CT = computed tomography.

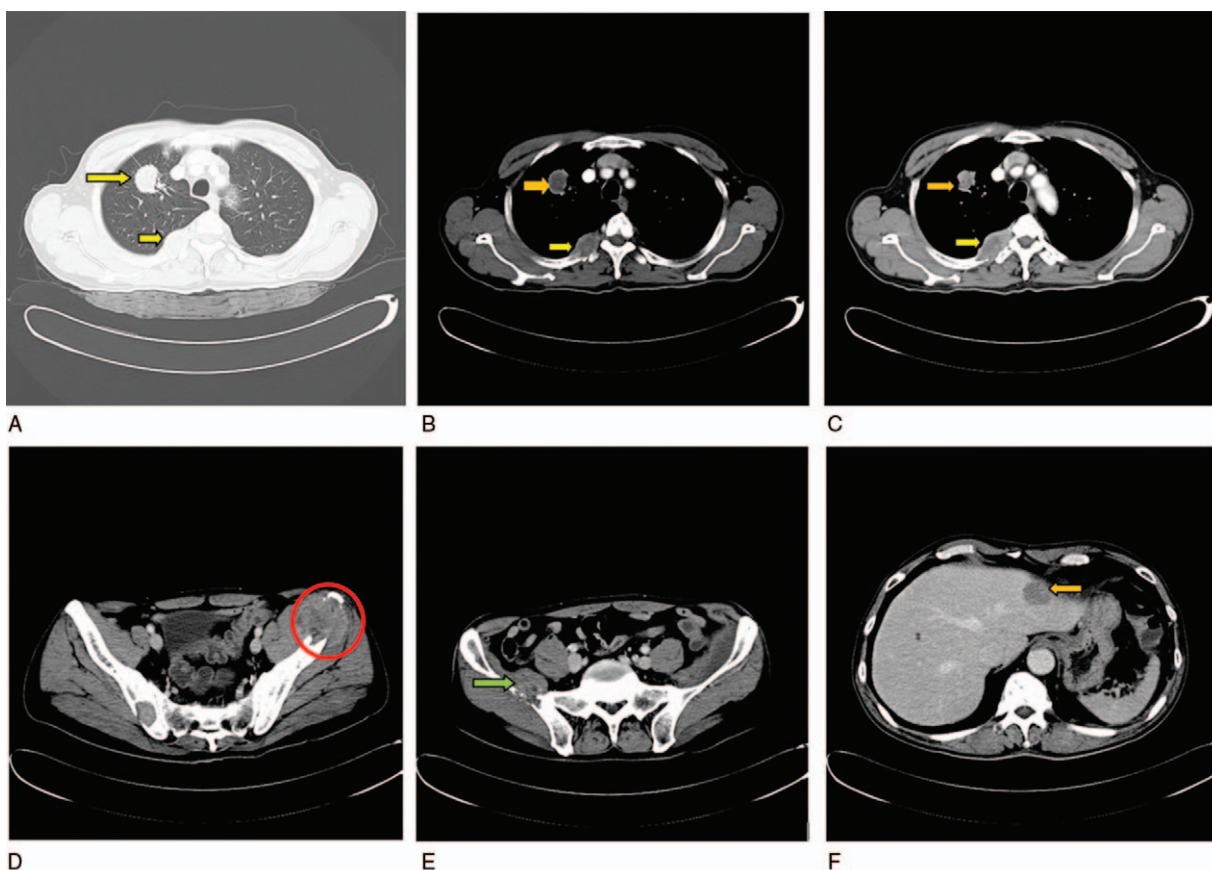


Figure 2. CT examination in our hospital on May 27, 2017. The upper lobe mass of the right lung, about 3.1×2.5 cm in size, is characterized by burrs and lobulations (A. lung window; B. mediastinum window; C. mediastinum window and contrast-enhanced). Both sides of iliac bone destruction and surrounding soft tissue swelling with a size of about 4.5×4.8 cm (D, right) and 3.2×2.0 cm (E, left). A slightly low-density nodule on the left lateral lobe of liver about 3.0×2.5 cm in size, and slightly enhanced by the contrast (F).

radiotherapy regimen changed. Target delineation: the CT imaging of right fourth rib metastases and the surrounding soft tissues was GTV3; CT imaging of the metastatic tumor of the cervical spine was GTV4. GTV3 and GTV4 expanded 5 and 3 cm were the pCTV3 and pCTV4, respectively. The CT imaging of the liver left lobe tumor was GTV5. GTV5 expanded 1 cm upwards and underneath and 0.7 cm on the other direction were the pCTV5. The dose of irradiation was pCTV3-5: 50 Gy/25f. pCTV3-5 radiotherapy was performed 14 times, but the patient's pain was not controlled well. CT re-examination on July 26, 2017 revealed the soft tissue masses around the 4th ribs were larger than when examined on May 2, 2017. Low density nodules in the left lateral lobe of the liver were enlarged to 5.2×3.3 cm (SIMA11) in size, and a new nodule with the diameter of 0.8 cm (SIMA9) was found in the left lateral lobe of the liver. The other images had little change compared with the previous CT (Fig. 6). The Response Evaluation Criteria in Solid Tumors (RECIST) assessment was PD and the patient was discharged from the hospital under his own insistence on July 31, 2017.

To seek the possibility of targeted therapy, the liver biopsy specimen of the patient was sent to Origimed on June 24, 2017. Of the 450 tumor related genes that were identified, 7 clinically significant genetic variants, including *MET* amplification, *STK11* M51fs*106 exon1, *KRAS* G12C exon2, *NCOR1* S1952*

exon37, *RBM10* E832* exon22, *SETD2* Q2030* exon13 and *SUFU* c.1022+1G>T, were detected. Based on the highest variation abundance of *STK11* M51fs*106 exon1, the patient was given 10 mg qd. po. everolimus on July 29, 2017 and had a dose adjustment to 250 mg bid. po. on September 3, 2017. During the whole course of treatment, the pain was not alleviated and his general condition continued to deteriorate until the patient finally died on October 17, 2017. This study was approved by the ethics committee of Affiliated Tumor Hospital of Guangxi Medical University (Ethical approval number: LW2018019). Informed consent for publication of the case has been obtained in writing from the deceased patient's next of kin.

3. Discussion

Urothelial carcinoma is the most common malignancy in the urinary system. It mostly invades the tissues and organs around the primary focus, and rarely metastasizes to distant organs. Bone (about 35%) is the most common distant metastatic organ in advanced urothelial carcinoma and the vertebrae is the most common site (about 40%) in all cases of bone metastasis.^[9] In our case, the first complaint of the patient was bone-ache, and further examination found that the urothelial carcinoma had occurred widely in bone metastases, which conformed with the general

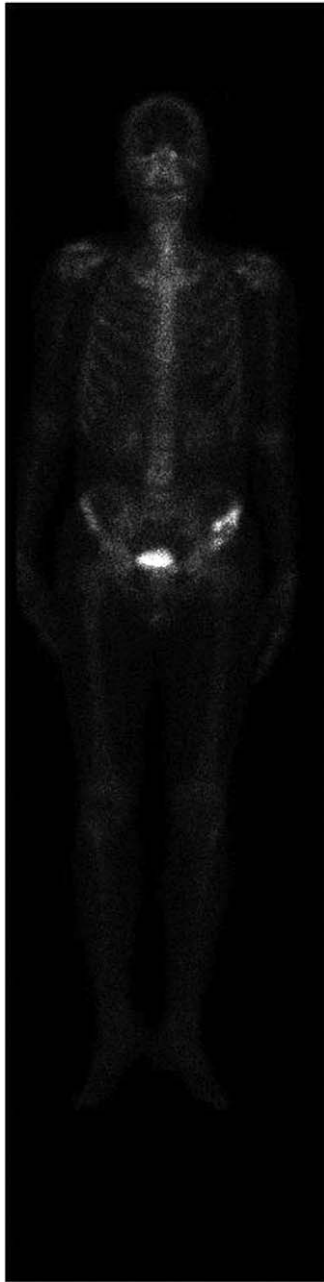


Figure 3. Whole-body bone scan by emission CT (ECT) in our hospital on June 1, 2017. Multiple spots and flaky radioactive concentrating foci could be seen on both sides of the iliac bone.

characteristics of urothelial carcinoma. However, it was quite rare to find metastatic lesions of bone, liver, and lung, rather than lesions of the urinary system.

Occult carcinoma cases have been described in breast, thyroid, and genitourinary system cancers (Table 1). Occult breast cancer accounts for 0.3% to 1% of all breast cancers, and the first manifestation is axillary nodal metastasis.^[10–13] Thus, it would be expected that occult primary breast cancer treatment would focus on local control of axillary disease, and the vast majority of patients underwent axillary lymph node dissection. Occult thyroid carcinoma includes papillary, follicular, and medullary carcinoma, with papillary carcinoma being the most common

subtype.^[14–17] It was reported that occult thyroid carcinoma is popular (with proportion of 36%) in autopsy specimens.^[14] Occult genitourinary system tumors mainly include ovarian, cervical, renal, and prostate cancer but are rarely reported. The incidence of sporadic multifocal renal cell carcinoma (both manifest and occult) ranges from 5.3% to 25% where occult multifocality accounts for the majority.^[18] Prevalence of occult prostate cancer is >30% in men over 50 years old and >60% to 70% in men over 80 years old.^[19] Clinical data suggest that >30% of men without prostate cancer history have occult prostate cancer.^[19] The major treatment for occult genitourinary system tumor is resection.^[20–22] As far as we know, this case is the first report of occult urothelial carcinoma. However, the biological mechanism of the unusual phenomenon is not clear yet. Occult carcinoma is different from that of the carcinoma of unknown primary (CUP). The former can identify the origin of the primary tissue or organ by pathological examination, whereas the CUP cannot. However, judging from this case, poor prognosis is a common challenge.^[23] Proper identification of the primary tumor origin is essential for determining a correct therapeutic strategy.

In addition, we acquired genetic alteration information of the cancer cells by next generation sequencing (NGS) analysis of the patient's liver cancer specimens. Seven genetic variants with clinical significance, including *MET* amplification, *STK11* M51Ifs*106 exon1, *KRAS* G12C exon2, *NCOR1* S1952* exon37, *RBM10* E832* exon22, *SETD2* Q2030* exon13, and *SUFU* c.1022+1G>T were detected in 450 cancer related genes.

Tyrosine kinase c-*MET*, encoded by the *METa* proto-oncogene, is a receptor of hepatocyte growth factor (HGF).^[24] C-*MET* is mainly expressed in epithelial cells, and its ligand HGF is expressed and released by surrounding mesenchymal cells.^[24] In a normal physiological state, the combination of HGF and c-*MET* can activate a variety of downstream signaling pathways, including RAS/RAF/MAPK, PI3K/Akt/mTOR, SRC/FAK, and JUN, which can lead to the cell cycle process, proliferation, movement and migration, survival and cell transformation.^[24] *MET* gene mutations or amplification have been found in many human cancers, most commonly seen in lung and breast cancer. It can activate c-*MET* signaling and promote uncontrolled cell proliferation and tumor metastasis.^[25,26] *MET* gene amplification is often found in metastatic tumors, suggesting that it mainly plays a role in the process of tumor metastasis.^[26,27] *MET* gene variation (amplification or mutation), combined with over-expression of the protein, occurs in about 2% to 10% of bladder cancer cases and is associated with bladder cancer metastasis and poor survival.^[28,29] In this report, the extensive multiple organ metastasis (including liver, bone, and lung) of occult urothelial carcinoma might be related to *MET* amplification. Abnormal activation of *MET* can be inhibited by specific targeted inhibitors, such as cabozantinib and crizotinib. Cabozantinib can inhibit the proliferation of gastric cancer cell lines with *MET* amplification, but it is not effective for cell lines without *MET* amplification.^[30] A lung adenocarcinoma patient carrying *MET* gene amplification and 14 exon skipping mutation achieved complete remission after being treated with cabozantinib.^[31]

The protein encoded by the *STK11* gene belongs to serine/threonine kinase family and functions as a tumor suppressor.^[32] In this report, the *STK11* M51Ifs*106 mutation can be described as the 51st codon of methionine changed into isoleucine and the 106th codon becoming a stop codon in the new open reading frame. This mutation caused premature termination codons

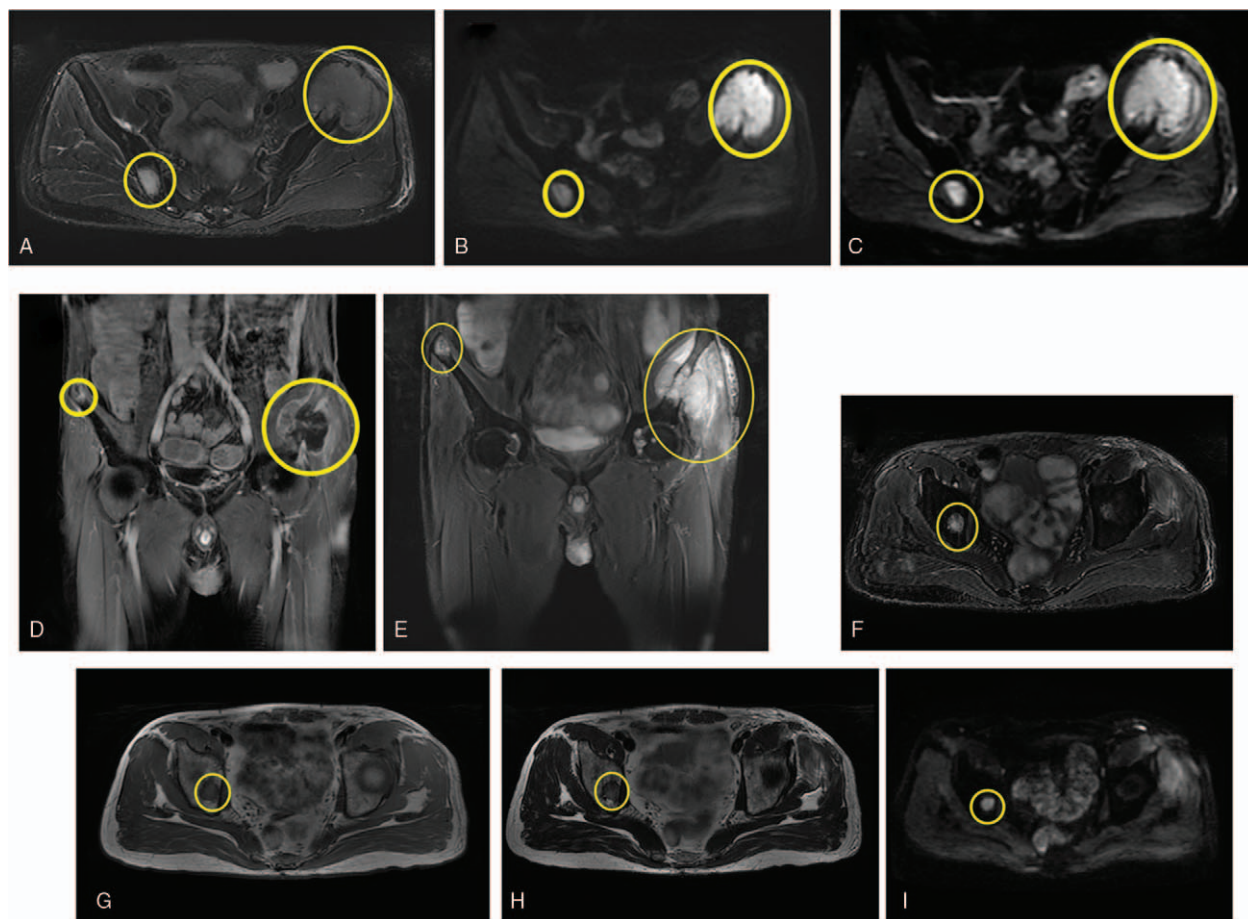


Figure 4. Magnetic resonance imaging of pelvis in our hospital on June 12, 2017. The fat suppression images indicated bilateral iliac bone destruction with soft tissue mass formation, with a size of about 5.8 × 6.7 cm (A. T2WI; B. DWI; C. T1WI). Coronal position images showed uneven contrast-enhancement of bilateral iliac lesions (D. pre-contrast; E. post-contrast). The fat suppression images indicated left acetabular lesion (F. T2WI; G. T1WI; H. T2WI contrast-enhanced; I. T1WI contrast-enhanced). DWI=diffusion-weighted imaging; T1WI=T1-weighted imaging; T2WI=T2-weighted imaging.

(PTCs) and produced new transcripts that can be degraded by an mRNA surveillance pathway termed nonsense-mediated mRNA decay (NMD). Although there are no anti-tumor drugs targeting the *STK11* gene, the inhibition of mTOR can be used as a treatment for cancer patients with *STK11* dysfunction. In the *STK11*^{-/-} mouse breast cancer tumor model, mTOR inhibitor AZD8055 can inhibit tumor growth successfully.^[33] A patient with metastatic atypical pituitary adenomas with *STK11* F298L variation was treated with radiotherapy and everolimus, and MRI and positron emission tomography and computed tomography showed stable disease (SD) over 6 months.^[34] Another study involving a Peutz-Jeghers syndrome associated advanced pancreatic cancer patient, achieved partial response (PR) with the treatment of everolimus.^[35] In this case, based on the mutation of *STK11* M51fs*106, the patient was treated with everolimus, but it was not very effective and the patient's condition continued to deteriorate. We considered that this might be due to the severity of illness. In addition, the patient carried a variety of tumor related gene mutations. Under these circumstances, choosing a treatment strategy with a combination (such as imimols + cabozantinib) or crizotinib alone still needs further study.

KRAS belongs to the RAS family and is one of the most mutated oncogenes in human tumors. *KRAS* mutations mainly

occur in the 12th, 13th and 61st codons, which may affect RAS mediated guanosine triphosphate (GTP) hydrolysis and lead to the continuous activation of RAS, promoting the malignant transformation of cells.^[36] G12C is one of the most common mutations in *KRAS* located in the 2nd exon. The glycine or proline of the 12' position can maintain the alpha helix structure in the GTP binding domain, which is crucial to inhibit the function of *KRAS* in promoting cell carcinogenesis.^[37] Compared with the mutation of position 13, the mutation of the 12th position has a stronger ability to resist cell death and promote transformation of cancer cells.^[38] Although there is no anti-tumor drug targeting the *KRAS* gene, MEK inhibitors and PI3K pathway inhibitors have a certain therapeutic effect in treating cancer patients with *KRAS* mutations.^[39]

Both enhanced and blocked functions of the *NCOR1* gene have been reported in tumors. The expression level of *NCOR1* protein in gastrointestinal stromal tumor is lower than that in normal gastric tissue, and it is significantly correlated with patient survival.^[40] However, in breast cancer, patients with a high expression of *NCOR1* have a better prognosis than those with low expression.^[41] In this case, the patient with occult urothelial carcinoma had a *NCOR1* S1952* mutation which resulted in protein truncation. The truncated *NCOR1* lost the functional

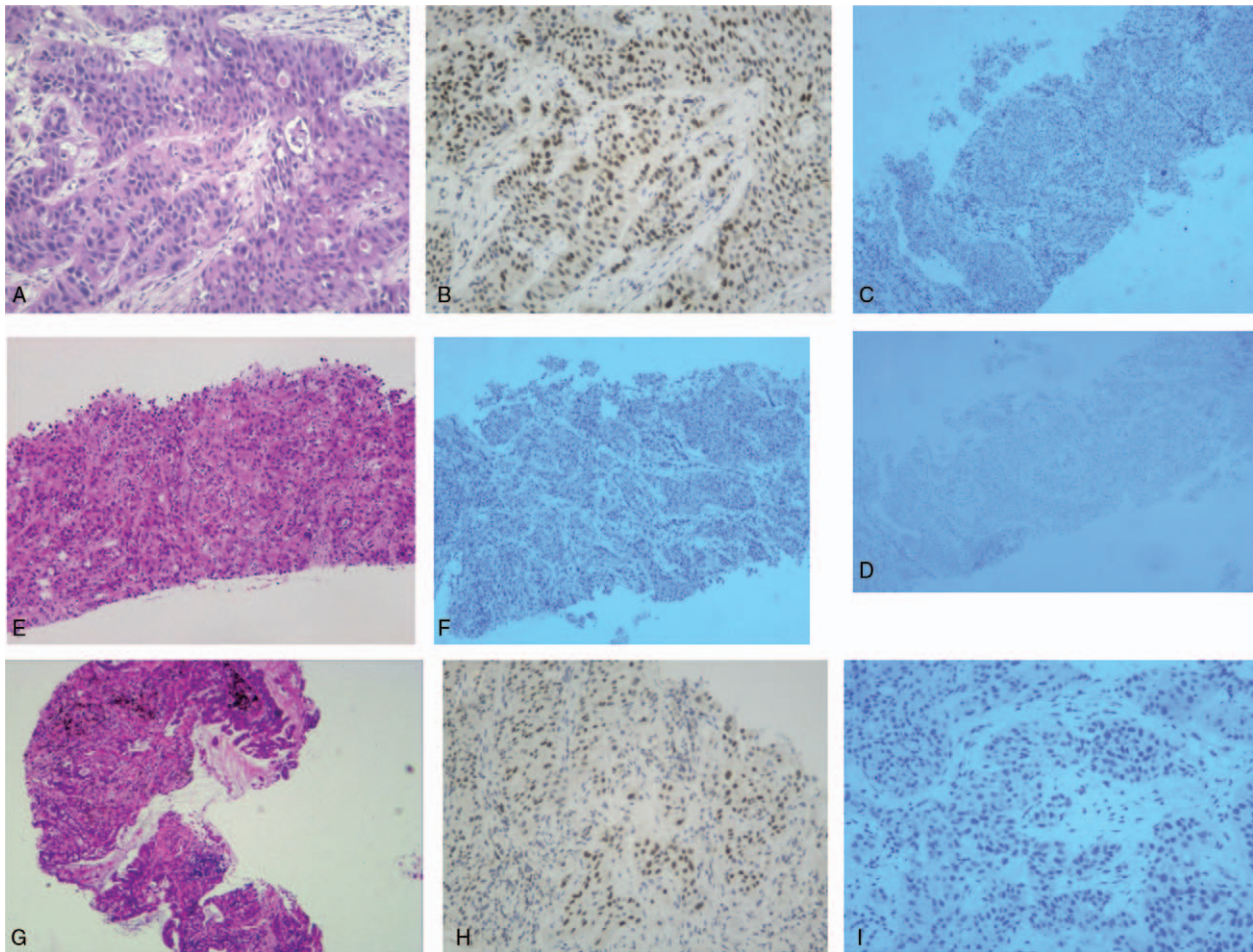


Figure 5. Pathological examination of biopsy specimens. Biopsy results for the left iliac bone. (A) H&E staining: the cells were arranged in sheets and variable in size, 200 \times ; IHC results: (B) Gata-3+ 200 \times ; (C) Villin- 100 \times ; (D) CDX2- 50 \times . Biopsy results for the liver. (E) H&E staining: the cells were arranged in sheets and variable in size, 200 \times ; IHC results: (F) Glypican3- 100 \times . Biopsy results for the lung. (G) H&E staining, 100 \times ; IHC results: (H) GATA-3 + partly 200 \times ; (I) TTF-1 - 200 \times . CDX2= homeobox protein CDX-2, GATA-3=GATA3 GATA binding protein 3, H&E=hematoxylin and eosin; IHC=immunohistochemistry; TTF-1=thyroid transcription factor 1.

domain of the C1D interaction zone, RARA interaction region, and ID1 and ID2 region, meaning that this mutation may affect the normal function of *NCOR1*. It was speculated that the expression or function of *NCOR1* may be inhibited during the development of urothelial carcinoma. Presently, there is not an anti-cancer drug targeting the *NCOR1* gene.

RBM10 encodes a RNA-binding protein and regulates the alternative splicing of *NUMB* which is the antagonizing modulator of the Notch signaling pathway, and displays negative effects on the proliferation of cancer cells. The deletion or mutation of *NUMB* frequently occurs in lung cancer.^[42] *RBM10* mutation often coexists with known drive gene mutations.^[43] In this case, the mutation of *RBM10* E832*, as a first reported novel mutation, produced a truncated protein, which lost the G-patch domain (858–904 amino acid residues). The mutation of *RBM10* E810*, which has been reported in lung adenocarcinoma, also produced a truncated protein with G-patch domain deletion.^[43] It was suggested that *RBM10* E832* might be a harmful mutation affecting the normal function of *RBM10* protein. To date, an anti-cancer drug targeting the *RBM10* gene has not been found.

The mutations or translocations of the histone methyltransferase *SETD2* are found in leukemia and solid tumors.^[44,45] There

are many variants of *SETD2* mutated at different sites in the same tumor and this will have a selective advantage in the process of renal cell carcinoma.^[46] In this case, the *SETD2* Q2030* mutation caused the glutamine of position 2030 mutated to stop codon. The C-terminal 2030–2564 amino acid residue of the truncated *SETD2* protein contains the region interacting with *POLR2A* (the 2457–2564 amino acid residue).^[47] It was suggested that the variation of *SETD2* Q2030* might affect the normal function of *SETD2*. There is no anti-cancer drug targeting the *SETD2* gene at present.

As a tumor suppressor, loss of function of *SUFU* can increase the activity of Hedgehog (Hh) signaling. Abnormal activation of the Hh pathway is associated with tumor formation in various tissues.^[48] *SUFU* c.1022+1G>T mutation makes the G base in the splicing donor site into a T, which might cause abnormal mRNA splicing. This mutation has been reported as either a germline mutation or a somatic variation in Gorlin syndrome 136 and medulloblastoma.^[49,50] Real-time reverse transcription polymerase chain reaction confirms that *SUFU* c.1022+1G>T mutation causes *SUFU* exon 8 skipping, and forms a stop codon in the 9th exon. This incomplete protein loses binding ability to *GLI* or *GLI2*, and results in the accumulation of *GLI* in the nucleus and,

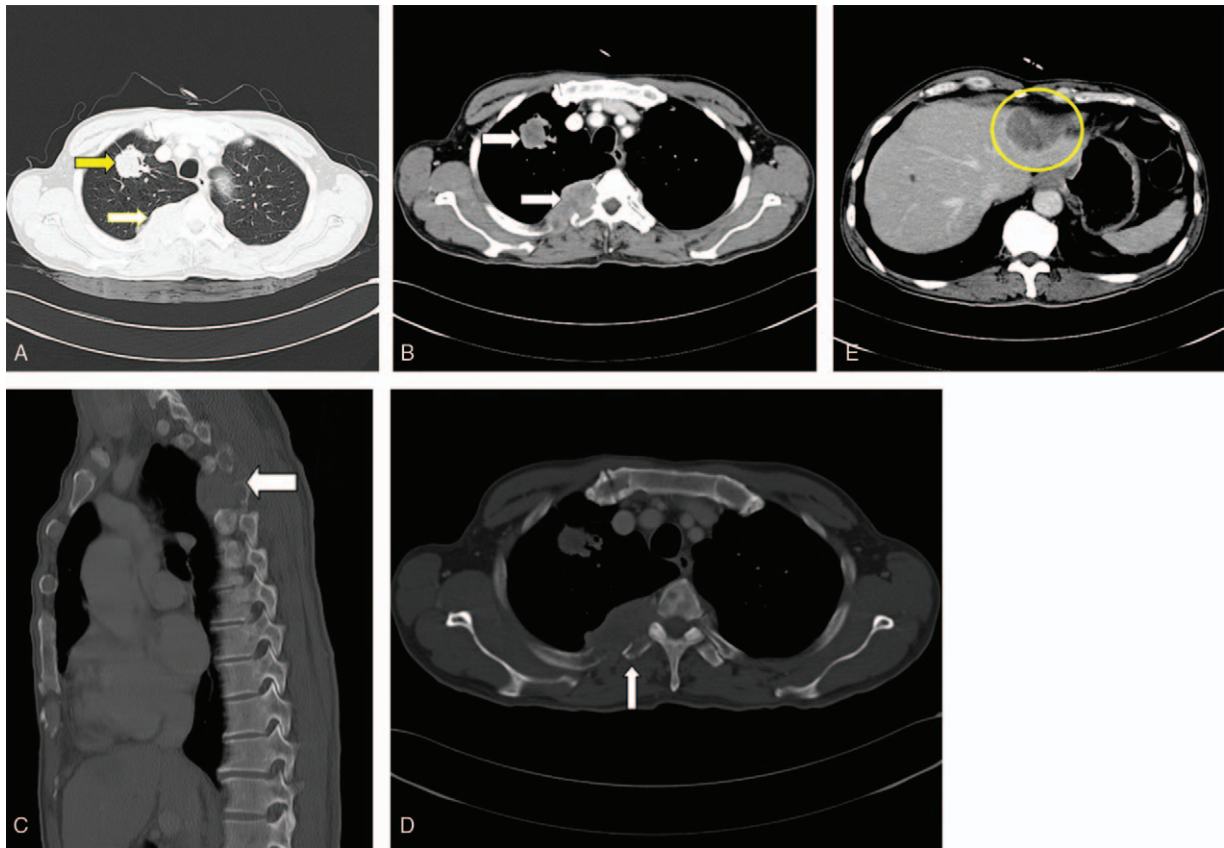


Figure 6. CT re-examination in our hospital on July 26, 2017. Compared with CT images on May 27, 2017, the size change of upper lobe mass of the right lung remained about the same (3.2 × 2.8 cm vs 3.1 × 2.5 cm. [A] Lung window; [B] mediastinum window). The bone destruction in the fourth sides of the right side, and the surrounding soft tissue mass increased (C and D). (E) The nodule on the left lateral lobe of liver was significantly larger than before (5.2 × 3.3 cm vs 3.0 × 2.5 cm). CT = computed tomography.

therefore, cannot inhibit GLI mediated transcriptional activation.^[50] There is no anti-cancer drug targeting the *SUFU* gene at present.

Based on gene test results, the patient was treated with everolimus, an inhibitor that indirectly targeted *STK11*, but the effect was poor. The patient’s condition continued to deteriorate until he passed away. This generates further questions as to

whether or not it is necessary to use a combination of targeted drugs for cancer patients with multiple genetic variants.

4. Conclusion

This patient was diagnosed with occult urothelial carcinoma by pathological evaluation and networking between the clinician

Table 1
Occult cancer data from previous reports.

| Age, y/Gender | Primary site | Metastatic site | Treatment | Outcome | Ref |
|---------------|--------------|--------------------------------------|--|---------|------|
| 42/Female | Breast | Axillary nodal | Modified radical mastectomy, hormonal therapy | Alive | [10] |
| 46/Female | Breast | Axillary nodal | Axillary lymph node dissection, chemotherapy | N/A | [11] |
| 59/Male | Breast | Axillary nodal | Mastectomy with axillary lymph node dissection, adjuvant chemotherapy | Alive | [12] |
| 45/Male | Breast | Axillary nodal | Axillary lymph node dissection, adjuvant radiation therapy, adjuvant chemotherapy | Alive | [12] |
| 47/Female | Breast | Gastroduodenal | Bilateral mastectomy with hormone therapy and chemotherapy | Alive | [13] |
| 60/Female | Ovarian | Bilateral supraclavicular lymph node | Bilateral salpingo-oophorectomy and cytoreductive surgery, chemotherapy | Dead | [20] |
| 43/Male | Prostate | Bilateral testicular | Bilateral orchiectomy, chemotherapy | Alive | [21] |
| 40/Male | Renal | N/A | Open radical nephrectomy | N/A | [22] |
| 54/Female | Thyroid | Lymph node | Thyroidectomy, bilateral modified neck dissections | Alive | [15] |
| 63/Female | Thyroid | Sacral, brain, chest and liver | Radioiodine | N/A | [16] |
| 61/Male | Thyroid | Pituitary and parotid | Palliative radiation and combination chemotherapy with capecitabine and temozolomide | Alive | [17] |

and pathologists. In addition, the 7 gene alterations of liver cancer tissue were detected by NGS analysis. From this case report, we can increase our knowledge of occult urothelial carcinoma and provide insight into combining multiple targeted drugs for the treatment of cancer patients with multiple driven genes.

Author contributions

Conceptualization: Bixun Li.

Data curation: Kunpeng Bu, Yang Lu, Juan Zhao.

Investigation: Kunpeng Bu, Yang Lu, Juan Zhao.

Supervision: Bixun Li.

Writing – original draft: Kunpeng Bu.

Writing – review & editing: Zeyan Shi.

References

- Le Chevalier T, Cvitkovic E, Caille P, et al. Early metastatic cancer of unknown primary origin at presentation. A clinical study of 302 consecutive autopsied patients. *Arch Intern Med* 1988;148:2035–9.
- Terada M, Adachi Y, Sawaki M, et al. Occult breast cancer may originate from ectopic breast tissue present in axillary lymph nodes. *Breast Cancer Res Treat* 2018;172:1–7.
- Daraki V, Koukouraki S, Velegarakis G, et al. Rare presentation of occult medullary carcinoma of the thyroid as a mediastinal mass. *Hormones (Athens)* 2012;11:210–4.
- Desai VB, Wright JD, Schwartz PE, et al. Occult gynecologic cancer in women undergoing hysterectomy or myomectomy for benign indications. *Obstet Gynecol* 2018;131:642–51.
- Bond LM, Skrobo D. Multiple embolic cerebral infarcts as the first manifestation of metastatic ovarian cancer. *BMJ Case Rep* 2015;2015: pii: bcr2015211521.
- Tsai CC, Wu MN. Frequent ischemic stroke as first manifestation of occult colon cancer: a rare case. *Am J Case Rep* 2015;16:723–7.
- Galimberti V, Bassani G, Monti S, et al. Clinical experience with axillary presentation breast cancer. *Breast Cancer Res Treat* 2004;88:43–7.
- Walker GV, Smith GL, Perkins GH, et al. Population-based analysis of occult primary breast cancer with axillary lymph node metastasis. *Cancer* 2010;116:4000–6.
- Punyavoravut V, Nelson SD. Diffuse bony metastasis from transitional cell carcinoma of urinary bladder: a case report and review of literature. *J Med Assoc Thai* 1999;82:839–43.
- Abe H, Naitoh H, Umeda T, et al. Occult breast cancer presenting axillary nodal metastasis: a case report. *Jpn J Clin Oncol* 2000;30:185–7.
- Altaha R, Abraham J. Paraneoplastic neurologic syndrome associated with occult breast cancer: a case report and review of literature. *Breast J* 2003;9:417–9.
- Hur SM, Cho DH, Lee SK, et al. Occult breast cancers manifesting as axillary lymph node metastasis in men: a two-case report. *J Breast Cancer* 2012;15:359–63.
- Zuhair AR, Maron AR. Occult bilateral invasive lobular carcinoma of the breast presenting as gastroduodenal metastases: a case report. *Breast Dis* 2015;35:63–5.
- Joshi P, Nair S, Nair D, et al. Incidence of occult papillary carcinoma of thyroid in Indian population: case series and review of literature. *J Cancer Res Ther* 2014;10:693–5.
- Saydam L, Kalcioğlu T, Demirkiran A, et al. Occult papillary thyroid carcinoma presenting as a parapharyngeal metastasis. *Am J Otolaryngol* 1999;20:166–8.
- Coban G, Yildirim E, Gemici K, et al. MRI findings of lumbosacral metastasis from occult follicular thyroid cancer: report of a case. *Surg Today* 2014;44:553–7.
- Conway A, Wiernik A, Rawal A, et al. Occult primary medullary thyroid carcinoma presenting with pituitary and parotid metastases: case report and review of the literature. *Endocr Pathol* 2012;23:115–22.
- Tsivian M, Moreira DM, Caso JR, et al. Predicting occult multifocality of renal cell carcinoma. *Eur Urol* 2010;58:118–26.
- Iguchi T, Wang CY, Delongchamps NB, et al. Occult prostate cancer effects the results of case-control studies due to verification bias. *Anticancer Res* 2008;28:3007–10.
- He S, Li P, Chen X, et al. Fluid biopsy for circulating tumor cells in an occult ovarian cancer patient exhibiting bilateral supraclavicular lymph node metastases: a case report. *Oncol Lett* 2013;6:448–52.
- Kamble VR, Agrawal PM. Bilateral testicular metastases from occult primary prostate cancer in a young adult: a rare case report. *J Clin Diagn Res* 2017;11:TD03–5.
- Ansari MS, Singh I, Gupta NP. Renal stone masquerading as an occult renal cell cancer (incidental RCC). *Int Urol Nephrol* 2004;36:235–7.
- Choi J, Nahm JH, Kim SK. Prognostic clinicopathologic factors in carcinoma of unknown primary origin: a study of 106 consecutive cases. *Oncotarget* 2017;8:62630–40.
- Organ SL, Tsao MS. An overview of the c-MET signaling pathway. *Ther Adv Med Oncol* 2011;3(1 suppl):S7–19.
- Bean J, Brennan C, Shih JY, et al. MET amplification occurs with or without T790M mutations in EGFR mutant lung tumors with acquired resistance to gefitinib or erlotinib. *Proc Natl Acad Sci USA* 2007;104:20932–7.
- Zeng ZS, Weiser MR, Kuntz E, et al. c-Met gene amplification is associated with advanced stage colorectal cancer and liver metastases. *Cancer Lett* 2008;265:258–69.
- An X, Wang F, Shao Q, et al. MET amplification is not rare and predicts unfavorable clinical outcomes in patients with recurrent/metastatic gastric cancer after chemotherapy. *Cancer* 2014;120:675–82.
- Iyer G, Al-Ahmadie H, Schultz N, et al. Prevalence and co-occurrence of actionable genomic alterations in high-grade bladder cancer. *J Clin Oncol* 2013;31:3133–40.
- Miyata Y, Sagara Y, Kanda S, et al. Phosphorylated hepatocyte growth factor receptor/c-Met is associated with tumor growth and prognosis in patients with bladder cancer: correlation with matrix metalloproteinase-2 and -7 and E-cadherin. *Hum Pathol* 2009;40:496–504.
- Yakes FM, Chen J, Tan J, et al. Cabozantinib (XL184), a novel MET and VEGFR2 inhibitor, simultaneously suppresses metastasis, angiogenesis, and tumor growth. *Mol Cancer Ther* 2011;10:2298–308.
- Paik PK, Drilon A, Fan PD, et al. Response to MET inhibitors in patients with stage IV lung adenocarcinomas harboring MET mutations causing exon 14 skipping. *Cancer Discov* 2015;5:842–9.
- Woods A, Johnstone SR, Dickerson K, et al. LKB1 is the upstream kinase in the AMP-activated protein kinase cascade. *Curr Biol* 2003;13:2004–8.
- Andrade-Vieira R, Goguen D, Bentley HA, et al. Pre-clinical study of drug combinations that reduce breast cancer burden due to aberrant mTOR and metabolism promoted by LKB1 loss. *Oncotarget* 2014;5:12738–52.
- Donovan LE, Arnal AV, Wang SH, et al. Widely metastatic atypical pituitary adenoma with mTOR pathway STK11(F298L) mutation treated with everolimus therapy. *CNS Oncol* 2016;5:203–9.
- Klumpfen HJ, Queiroz KC, Spek CA, et al. mTOR inhibitor treatment of pancreatic cancer in a patient with Peutz-Jeghers syndrome. *J Clin Oncol* 2011;29:e150–3.
- Birkeland E, Wik E, Mjos S, et al. KRAS gene amplification and overexpression but not mutation associates with aggressive and metastatic endometrial cancer. *Br J Cancer* 2012;107:1997–2004.
- Seeburg PH, Colby WW, Capon DJ, et al. Biological properties of human c-Ha-ras1 genes mutated at codon 12. *Nature* 1984;312:71–5.
- Guerrero S, Casanova I, Farre L, et al. K-ras codon 12 mutation induces higher level of resistance to apoptosis and predisposition to anchorage-independent growth than codon 13 mutation or proto-oncogene overexpression. *Cancer Res* 2000;60:6750–6.
- Engelman JA, Chen L, Tan X, et al. Effective use of PI3K and MEK inhibitors to treat mutant Kras G12D and PIK3CA H1047R murine lung cancers. *Nat Med* 2008;14:1351–6.
- Wang W, Song XW, Bu XM, et al. PDCD2 and NCoR1 as putative tumor suppressors in gastric gastrointestinal stromal tumors. *Cell Oncol (Dordr)* 2016;39:129–37.
- Lavinsky RM, Jepsen K, Heinzl T, et al. Diverse signaling pathways modulate nuclear receptor recruitment of N-CoR and SMRT complexes. *Proc Natl Acad Sci USA* 1998;95:2920–5.
- Bechara EG, Sebestyen E, Bernardis I, et al. RBM5, 6, and 10 differentially regulate NUMB alternative splicing to control cancer cell proliferation. *Mol Cell* 2013;52:720–33.
- Imielinski M, Berger AH, Hammerman PS, et al. Mapping the hallmarks of lung adenocarcinoma with massively parallel sequencing. *Cell* 2012;150:1107–20.

- [44] Zhang J, Ding L, Holmfeldt L, et al. The genetic basis of early T-cell precursor acute lymphoblastic leukaemia. *Nature* 2012;481:157–63.
- [45] Al Sarakbi W, Sasi W, Jiang WG, et al. The mRNA expression of SETD2 in human breast cancer: correlation with clinico-pathological parameters. *BMC Cancer* 2009;9:290.
- [46] Gerlinger M, Rowan AJ, Horswell S, et al. Intratumor heterogeneity and branched evolution revealed by multiregion sequencing. *N Engl J Med* 2012;366:883–92.
- [47] Li M, Phatnani HP, Guan Z, et al. Solution structure of the Set2-Rpb1 interacting domain of human Set2 and its interaction with the hyperphosphorylated C-terminal domain of Rpb1. *Proc Natl Acad Sci USA* 2005;102:17636–41.
- [48] Scales SJ, de Sauvage FJ. Mechanisms of Hedgehog pathway activation in cancer and implications for therapy. *Trends Pharmacol Sci* 2009;30:303–12.
- [49] Pastorino L, Giorzo P, Nasti S, et al. Identification of a SUFU germline mutation in a family with Gorlin syndrome. *Am J Med Genet A* 2009;149A:1539–43.
- [50] Taylor MD, Liu L, Raffel C, et al. Mutations in SUFU predispose to medulloblastoma. *Nat Genet* 2002;31:306–10.